applied sciences

MDPI

Article

Adjustment of Terahertz Properties Assigned to the First Lowest Transition of (D^+, X) Excitonic Complex in a Single Spherical Quantum Dot Using Temperature and Pressure

Noreddine Aghoutane [1], Laura M. Pérez [2], Anton Tiutiunnyk [2], David Laroze [2], Sotirios Baskoutas [3,*], Francis Dujardin [4], Abdelouahad El Fatimy [5,6], Mohamed El-Yadri [1] and El Mustapha Feddi [1,*]

1 Group of Optoelectronic of Semiconductors and Nanomaterials, ENSAM, Mohammed V University in Rabat, Rabat 10100, Morocco; noreddine.aghoutane@gmail.com (N.A.); mohamed.elyadri@um5.ac.ma (M.E.-Y.)
2 Instituto de Alta Investigación, CEDENNA, Universidad de Tarapacá, Casilla 7 D, Arica 1000000, Chile; lperez@uta.cl (L.M.P.); tyutyunnyk.a.m@gmail.com (A.T.); dlarozen@uta.cl (D.L.)
3 Department of Materials Science, University of Patras, GR-26504 Patras, Greece
4 Laboratoire de Chimie et Physique-Approche Multi-échelles des Milieux Complexes, Université de Lorraine, LCP-A2MC, F-57000 Metz, France; francis.dujardin@univ-lorraine.fr
5 Central European Institute of Technology, Brno University of Technology, 60190 Brno, Czech Republic; a.elfatimy@gmail.com
6 Département de physique, Ecole Centrale Casablanca , Bouskoura, Ville Verte, Casablanca 27182, Morocco
* Correspondence: bask@upatras.gr (S.B.); e.feddi@um5s.net.ma (E.M.F.)

check for updates

Citation: Aghoutane, N.; Pérez, L.M.; Tiutiunnyk, A.; Laroze, D.; Baskoutas, S.; Dujardin, F.; El Fatimy, A.; El-Yadri, M.; Feddi, E.M. Adjustment of Terahertz Properties Assigned to the First Lowest Transition of (D^+, X) Excitonic Complex in a Single Spherical Quantum Dot Using Temperature and Pressure. *Appl. Sci.* **2021**, *11*, 5969. https://doi.org/10.3390/app11135969

Academic Editors: Alessandro Sergi and Gabriel Hanna

Received: 20 May 2021
Accepted: 23 June 2021
Published: 27 June 2021

Publisher's Note: MDPI stays neutral with regard to jurisdictional claims in published maps and institutional affiliations.

Copyright: © 2021 by the authors. Licensee MDPI, Basel, Switzerland. This article is an open access article distributed under the terms and conditions of the Creative Commons Attribution (CC BY) license (https://creativecommons.org/licenses/by/4.0/).

Abstract: This theoretical study is devoted to the effects of pressure and temperature on the optoelectronic properties assigned to the first lowest transition of the (D^+, X) excitonic complex (exciton-ionized donor) inside a single $AlAs/GaAs/AlAs$ spherical quantum dot. Calculations are performed within the effective mass approximation theory using the variational method. Optical absorption and refractive index as function of the degree of confinement, pressure, and temperature are investigated. Numerical calculation shows that the pressure favors the electron-hole and electron-ionized donor attractions which leads to an enhancement of the binding energy, while an increasing of the temperature tends to reduce it. Our investigations show also that the resonant peaks of the absorption coefficient and the refractive index are located in the terahertz region and they undergo a shift to higher (lower) therahertz frequencies when the pressure (temperature) increases. The opposite effects caused by temperature and pressure have great practical importance because they offer an alternative approach for the adjustment and the control of the optical frequencies resulting from the transition between the fundamental and the first excited state of exciton bound to an ionized dopant. The comparison of the optical properties of exciton , impurity and (D^+, X) facilitates the experimental identification of these transitions which are often close. Our investigation shows that the optical responses of (D^+, X) are located between the exciton (high energy region) and donor impurity (low energy region) peaks. The whole of these conclusions may lead to the novel light detector or source of terahertz range.

Keywords: terahertz properties; quantum dots; (D^+, X) complex; temperature; pressure

1. Introduction

Quantum dots (QD) are considered as among important nanomaterials who are already entering the industry of the future [1,2]. Based on their fascinating physical properties due to the quantum confinement, these nanoforms of semiconductor materials are very usable for manufacturing a new generation of optoelectronic devices such as lasers, terahertz detectors, solar cells, LEDs, diodes, and transistors [3,4]. Among the important optical properties in such nanostructures are attributed to excitonic complexes transitions such as exciton X, biexciton X_2, exciton bound to a donor (D^0, X), exciton bound to an acceptor (A^0, X) and exciton bound to an ionized donor (D^+, X). Whether in bulk or confined

medium, numerous experimental and theoretical research have studied and identified the spectral lines attributed to these transitions [5–10].

One of the most interesting and fascinating complexes is (D^+, X), which is formed by the Coulomb interactions between an ionized donor, one hole, and one electron (D^+, e, h). Thus, it admits two possible paths for its formation or even for its dissociation $(D^+, X) \rightarrow D^+ + X$ or $(D^+, X) \rightarrow D^0 + h$. Stébé et al. [11] have discussed its stability in spherical quantum dots and demonstrated that the first process is more stable. In the last few years, we have developed many theoretical studies concerning the identification of the spectral lines of this complex using an electric field and comparing the Stark shift [12]. More recently, the effects of the magnetic field and host dielectric environment on the (D^+, X) binding energy has been analysed [13]. The comparison between the two protocols of dissociation has been studied and analysed deeply by considering the binding energy and optical absorption [14]. We have found considerable investigations on optical properties in literature, for more detail we refer the reader to some interesting manuscripts [15–25]. Recently we have studied the non-linear optical properties of an exciton confined in different QD shapes taking into account the pressure (P) and temperature (T) effects. We have shown that all these properties are deeply dependent on these external perturbations [26–28].

Related to our current work, there is a few studies which have treated the optical properties of the (D^+, X) complex. The most important of them concerns the oscillator strength related to the intersubband transition in a disc-like parabolic QD as function of the frequency of the parabolic confining potential [29]. Xie et al. [30] also analysed the effects of T and P on the absorption properties of an exciton-donor complex in a disc-shaped quantum dot with Gaussian potential. Other interesting studies are those done by Z. Dongmei et al. [31] who calculated the optical properties of (D^+, X) confined in strained wurtzite $ZnO/Mg_{0.25}Zn_{0.75}O$ quantum dots. They have found that the absorption coefficient peak presents a blueshift for strong confinement. At last, an investigation was done by L. Dallali et al. [32], which concerns a comparison of optoelectronic properties of exciton, donor and acceptor exciton complexes, (D^+, X) and (A^-, X) respectively, in ZnO/SiO_2. They have shown that their optical transition energies and binding energy are dependent on both the dot sizes and the type of the impurities in interaction with exciton. To discover some particularities related to the optical transition between the lowest states $1s$ and $1p$ of the exciton bound to an ionized donor, we report in this paper a full theoretical analysis of the linear and non-linear optical properties associated to the existence of this entity. Our investigation will consider the effects of QD sizes, temperature and pressure. Thus, we will analyse the behaviours of the change of the refractive indexes (RI) and the linear and non-linear absorption coefficients (AC) variations involving the first allowed transition $(1s - 1p)$. For a better comprehension of the phenomenon, we compare all (D^+, X) peaks with those obtained for the exciton and impurity. After this introduction, in Section 2 is provided a detailed theoretical method. The results are discussed in Section 3, and the final remarks are given in Section 4.

2. Background Theory

Let us consider an exciton, $X(e, h)$, bound to an ionized donor impurity (D^+) confined in a single $GaAs$ spherical quantum dot $(SSQD)$ embedded in a glass matrix or host material with large band gap. The system formed (D^+, X) is similar to the Helium like-atom which constitute a physical three bodies problem. To reduce the number of variables, we suppose that the ionized donor is located at the centre of the $SSQD$. Within the framework of the effective mass approximation and considering the thermal and strain effects, the Hamiltonian of (D^+, X) complex can be written as:

$$\mathcal{H} = -\frac{\hbar^2}{2\, m_e^*(P,T)}\Delta_e - \frac{\hbar^2}{2\, m_h^*(P,T)}\Delta_h - \frac{e^2}{\varepsilon(P,T)}\left(\frac{1}{r_e} + \frac{1}{r_{eh}} - \frac{1}{r_h}\right) + V_w^e + V_w^h, \quad (1)$$

where $r_{eh} = \left|\overrightarrow{r_e} - \overrightarrow{r_h}\right|$ is the electron to hole distance. $\varepsilon(P,T)$, $m_e^*(P,T)$ and $m_h^*(P,T)$ are the dielectric constant, electron and hole effective masses, respectively. All these parameters depend on the temperature T, and pressure P. They can be expressed by the following variation laws [33,34]:

$$\varepsilon(P,T) = \begin{cases} 12.7\exp(-1.67\times10^{-3}P)\exp(9.4\times10^{-5}(T-75.6)) \\ \text{for } 0 \le T \le 200\ K \\ 13.18\exp(-1.73\times10^{-3}P)\exp(20.4\times10^{-5}(T-300)) \\ \text{for } T > 200\ K \end{cases} \tag{2}$$

$$m_e^*(P,T) = m_0\left(1 + 7.51\left(\frac{2}{E_g(P,T)} + \frac{1}{E_g(P,T)+\Delta_0}\right)\right)^{-1} \tag{3}$$

and

$$m_h^*(P,T) = m_0\Big(0.09 - 0.2\times10^{-3}P - 3.55\times10^{-5}T\Big), \tag{4}$$

where Δ_0 is the spin-orbit splitting. Here, the band gap $E_g(P,T)$ is given by the Varshni relation [33,35]:

$$E_g(P,T) = 1.519 - \frac{5.4\times10^{-4}\ T^2}{T+204} + 0.01261\ P + 3.77\times10^{-5}P^2. \tag{5}$$

In glass matrix or in other medium with large band gap, the confinement relative to a $SSQD$ can be described by [12–14] :

$$V_w^i(r_i) = \begin{cases} 0 & inside \\ \infty; & outside \end{cases} \quad i = (e,h). \tag{6}$$

On the other hand, under strain effect, the radius of the $SSQD$ can be obtained by applying the strain tensor components of spherical dot radius [36]:

$$R(P) = R(0)[1 - (S_{11} + 2S_{12})P]^{1/3} \tag{7}$$

where $R(0)$ is the unstrained $SSQD$ size and S_{11} and S_{12} are the compliance parameters obtained using the elastic constant C_{11} and C_{12} such as [16,37,38]:

$$S_{11} = \frac{C_{11} + C_{12}}{(C_{11} - C_{12})(C_{11} + 2C_{12})} \tag{8}$$

and

$$S_{12} = \frac{C_{12}}{(C_{11} - C_{12})(C_{11} + 2C_{12})}. \tag{9}$$

By using the effective units, $a_D = \varepsilon_0\hbar^2/m_e^*e^2$ for length and $R_D = \hbar^2/m_e^*a_D^2$ for energy, the Hamiltonian given in Equation (1) can be written as:

$$\mathcal{H} = \frac{m_e^*}{2}\left(-\frac{1}{m_e^*(P,T)}\Delta_e - \frac{1}{m_h^*(P,T)}\Delta_h - \frac{\varepsilon_0}{\varepsilon(P,T)}\left(\frac{1}{r_e} + \frac{1}{r_{eh}} - \frac{1}{r_h}\right)\right). \tag{10}$$

In such a situation, the Hylleraas coordinates $(r_e, r_h, r_{eh}, z_e, z_h)$ are the best coordinate system that can be used [39]. Thus, the Laplacian operator can be simply written in the following form:

$$\Delta_e = -\frac{\partial^2}{\partial r_e^2} - \frac{\partial^2}{\partial r_{eh}^2} - \left(\frac{r_e^2 - r_h^2 + r_{eh}^2}{r_e r_{eh}}\right)\frac{\partial^2}{\partial r_e \partial r_{eh}} - \frac{2}{r_e}\frac{\partial}{\partial r_e} - \frac{2}{r_{eh}}\frac{\partial}{\partial r_{eh}}. \quad (11)$$

Note that Δ_h can be obtained by interchanging e and h. The Schrödinger equation $\mathcal{H}\ \Psi^{(D^+,X)} = E_{(D^+,X)}\ \Psi^{(D^+,X)}$ does not admit an exact solution, so only a numerical approach can determine the lowest energy states. In order to solve this equation, we use a variational calculation based on a good choice of wave function and a minimization of the Hamiltonian mean value $< \mathcal{H} >$.

$$E_{(D^+,X)} = \min \frac{< \Psi|\mathcal{H}|\Psi >}{< \Psi|\Psi >}, \quad (12)$$

In our last sudies [25,40], we have demonstrated that the lowest states (n,l,m) of neutral donor (D^0) in spherical QDs correspond to $1s$ (1,0,0) and $1p$ (1,1,0) states. The same concept is used in order to built the variational wave functions of the (D^+, X) complex. In these conditions, the trial wave function of the (D^+, X) for the fundamental state ($1s$) is taken as:

$$\Psi_{1s}^{(D^+,X)} = A_0\, j_0(r_e)\, j_0(r_h) Y_0^0(\theta_e, \varphi_e) Y_0^0(\theta_h, \varphi_h)\, e^{-\beta_{1s} r_e - \eta_{1s} r_{eh}} \quad (13)$$

while the first excited state trial wave function $1p$ is taken as:

$$\Psi_{1p}^{(D^+,X)} = A_1\, j_1(r_e)\, j_1(r_h) r_e r_h Y_1^0(\theta_e, \varphi_e) Y_1^0(\theta_h, \varphi_h)\, e^{-\beta_{1p} r_e - \eta_{1p} r_{eh}} \quad (14)$$

A_0 and A_1 are the normalization constants. $j_0(r_i) = \frac{\sin(\pi r_i/R)}{r_i}$ and $j_1(r_i) = \frac{\sin(\varkappa r_i/R)}{(\varkappa r_i)^2} - \frac{\cos(\varkappa r_i/R)}{\varkappa r_i}$ $(i = e, h)$ are the first and second order of the the first kind of Bessel function respectively [41]. They represent the two first states obtained analytically by solving the Schrödinger equation of one particle in spherical QD. $Y_0^0(\theta_i, \varphi_i) = 1/\sqrt{\frac{1}{4\pi}}$ and $Y_1^0(\theta_i, \varphi_i) = \sqrt{\frac{3}{4\pi}}\cos(\theta_i)$ are the spherical harmonics for the fundamental and the first excited states respectively. The exponential factors $e^{-\beta_i r_e}$ and $e^{-\eta_i r_{eh}}$ $(i = 1s, 1p)$ traduce the Coulomb interactions of the electron with the ionized donor and the hole respectively. The β_i and η_i are variational parameters. We underline that in the $1p$ state, $j_1(r_i)$ represents the radial polynomial resulting from the resolution of the Schrödinger equation of Hydrogen-like atom. In these conditions, the energies are obtained by minimizing the mean value (12) by respect to the parameters β_i, η_i .

Furthermore, to compare the optical properties behaviour of (D^+, X) with the exciton X and the neutral donor D^0 (donor is fixed on the sphere center), it is necessary to follow the same method to determine the ground and first excited states energies of X and D^0 with the same accuracy as that of the complex (D^+, X). To this purpose we have performed variational calculations for both X and D^0 using the following trial wave functions:

$$\Psi_{1s}^{X} = A_0\, j_0(r_e)\, j_0(r_h) Y_0^0(\theta_e, \varphi_e) Y_0^0(\theta_h, \varphi_h)\, e^{-\gamma_{1s} r_{eh}} \quad (15)$$

$$\Psi_{1p}^{X} = A_1\, j_1(r_e)\, j_1(r_h) Y_1^0(\theta_e, \varphi_e) Y_1^0(\theta_h, \varphi_h) r_e r_h e^{-\gamma_{1p} r_{eh}} \quad (16)$$

for the exciton and

$$\Psi_{1s}^{D^0} = A_0\, j_0(r_e) Y_0^0(\theta_e, \varphi_e)\, e^{-\delta_{1s} r_e} \quad (17)$$

$$\Psi_{1p}^{D^0} = A_1\, j_1(r_e)\, Y_1^0(\theta_e, \varphi_e) r_e e^{-\delta_{1p} r_e} \quad (18)$$

for the donor impurity. We note that in these cases the Coulomb potentials are given by $V_c = -1/r_{eh}$ and $V_c = -1/r_e$ for X and D^0, respectively.

On the other hand, linear and non-linear optical properties are given in non-linear optical theory [42–49] in which the total refractive index changes (RIC), n_r, can be written as:

$$\frac{\Delta n(\omega, I)}{n_r} = \frac{\Delta^{(1)} n(\omega)}{n_r} + \frac{\Delta^{(3)} n(\omega, I)}{n_r}, \tag{19}$$

where

$$\frac{\Delta^{(1)} n(\omega)}{n_r} = \frac{1}{2\varepsilon_0 n_r^2} \frac{\sigma |M_{fi}|^2 (E_{fi} - \hbar\omega)}{(E_{fi} - \hbar\omega)^2 + (\hbar\Gamma_{fi})^2}, \tag{20}$$

and

$$\frac{\Delta^{(3)} n(\omega, I)}{n_r} = -\frac{\mu c I \sigma |M_{fi}|^4}{\varepsilon_0 n_r^3} \frac{(E_{fi} - \hbar\omega)}{\left[(E_{fi} - \hbar\omega)^2 + (\hbar\Gamma_{fi})^2\right]^2}$$
$$\left[1 - \frac{(M_{ff} - M_{ii})^2}{4|M_{fi}|^2 (E_{fi}^2 + (\hbar\Gamma_{fi})^2)} \left\{ E_{fi}(E_{fi} - \hbar\omega) - (\hbar\Gamma_{fi})^2 - (\hbar\Gamma_{fi})^2 \frac{(2E_{fi} - \hbar\omega)}{(E_{fi} - \hbar\omega)} \right\}\right] \tag{21}$$

Here, $E_{fi} = E_f - E_i$ corresponds to the energy of transition between $1p$ and $1s$ states, $M_{fi} = e\langle \Psi_i | \overrightarrow{r_e} - \overrightarrow{r_h} | \Psi_f \rangle = e\langle \Psi_i | r_{eh} | \Psi_f \rangle$ is the dipolar matrix element for light polarization, c is the speed of light in vacuum, σ is the electron density in the occupied volume ($\sigma = n/V(P)$), ε_0 is the vacuum permittivity, μ is the permeability of $GaAs$, $\hbar\omega$ is the incident photon energy, Γ_{fi} is the non-diagonal matrix element defined as inverse of the relaxation rate $\Gamma_{fi} = 1/\tau_{fi}$ and finally I is the intensity of the incident radiation.
At last, the total absorption coefficient can be deduced from the same formalism,

$$\alpha(\omega, I) = \alpha^{(1)}(\omega) + \alpha^{(3)}(\omega, I), \tag{22}$$

where

$$\alpha^{(1)}(\omega) = \omega \sqrt{\frac{\mu}{\varepsilon}} \frac{\sigma \hbar \Gamma_{fi} |M_{fi}|^2}{(E_{fi} - \hbar\omega)^2 + (\hbar\Gamma_{fi})^2}, \tag{23}$$

and

$$\alpha^{(3)}(\omega, I) = -\omega \sqrt{\frac{\mu}{\varepsilon}} \left(\frac{I}{2\varepsilon_0 n_r c}\right) \frac{4\sigma\hbar\Gamma_{fi}|M_{fi}|^4}{\left[(E_{fi} - \hbar\omega)^2 + (\hbar\Gamma_{fi})^2\right]^2}$$
$$\left[1 - \frac{\left|M_{ff} - M_{ii}\right|^2}{4|M_{fi}|^2} \frac{3E_{fi}^2 - 4\hbar\omega E_{fi} + \hbar^2(\omega^2 - \Gamma_{fi}^2)}{E_{fi}^2 + (\hbar\Gamma_{fi})^2}\right]. \tag{24}$$

In the next section, we present the corresponding numerical results.

3. Results and Discussions

Before presenting the behaviour of optical properties, we will focus on the influence of size, pressure, and temperature on the binding energy of the (D^+, X) complex confined in a $GaAs$ $SSQD$. All parameters used in our calculation are given in Table 1.

Table 1. Physical parameters of $GaAs$ and light properties [50].

$m_e^* = 0.067\ m_0$	$m_h^* = 0.079\ m_0$
$E_g = 1.607\,\text{eV}$	$\varepsilon = 13.18$
$\sigma = 3 \times 10^{22}\ \text{m}^{-3}$	$\Delta_0 = 0.341\,\text{eV}$
$n = 3.2$	$\Gamma_{fi} = 0.2\ \text{ps}^{-1}$
$S_{11} = 1.16 \times 10^{-2}\ \text{GPa}^{-1}$	$a_D = 10.41\ \text{nm}$
$S_{12} = -3.7 \times 10^{-3}\ \text{GPa}^{-1}$	$R_D = 10.5\ \text{meV}$
$I = 200\ \text{MW/m}^2$	

In our previous work [14] we have demonstrated that the most probable dissociation process of the (D^+, X) complex is : $(D^+, X) \rightarrow D^+ + X$. This is why it is more convenient to analyse this stability by defining the binding energy $E^b_{(D^+,X)}(P,T)$ as the difference of the correlated and non-correlated charge carriers: $E^b_{(D^+,X)}(P,T) = E_e(P,T) + E_h(P,T) - E_{(D^+,X)}(P,T)$, where E_h and E_e are the confined energies of single hole and electron respectively. $E_{(D^+,X)}(P,T)$ is the total energy of (D^+, X) complex obtained by minimization. According to this definition, we present in Figure 1a,b the contour plot of the (D^+, X) complex binding energy as function of pressure and temperature for two confinement regimes, $R = 2\ a_D$ and $3\ a_D$ respectively.

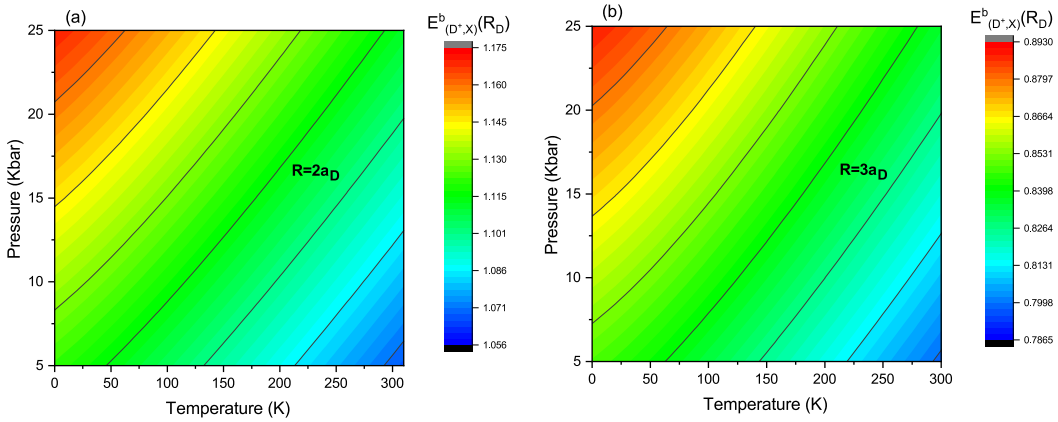

Figure 1. Binding energy variation of an exciton bound to an ionized donor as a function of pressure and temperature for the radius $R = 2a_D$ (**a**) and $R = 3a_D$ (**b**).

As a first remark, when the pressure is applied, we observe an increase in binding energy for both types of confinements. This growth is slightly sensitive to pressure for $R = 2\ a_D$ due to the fact that the strong confinement is predominant and the (D^+, X) complex is not influenced by this external perturbation. For $R = 3\ a_D$ the effect becomes significant. This is because in the case of weak confinement, the wave function is more extensive, and the charge carriers become more sensitive to the effect of pressure. Indeed, when the pressure increases, the dot size reduces which leads to a strong localization of the electronic density around the ionized donor, and therefore the pressure effect becomes more remarkable. To confirm this interpretation, the fit of our numerical results concerning the variation of $E^b_{(D^+,X)}$ as function of pressure leads to an interesting law:

$$E^b_{(D^+,X)}(P) = E^b_{(D^+,X)}(0) + 0.00239P.$$

From these curves we can see also, that $E^b_{(D^+,X)}$ decreases when temperature (T) increases, because the T tends to reduces the Coulomb interaction between the opposite charges in (D^+, X) what leads to loss of the stability of complex i.e. an increase of the temperature leads to significant decrements of the geometrical confinement contribution in the (D^+, X) binding energy. The variation of $E^b_{(D^+,X)}$ according to the temperature follows

the law: $E^b_{(D^+,X)}(T) = E^b_{(D^+,X)}(0) - 0.00178\ T$. Furthermore, looking at these behaviours, we see clearly that pressure and temperature generate two antagonistic effects which allow the control of transition energies without modify the sizes.

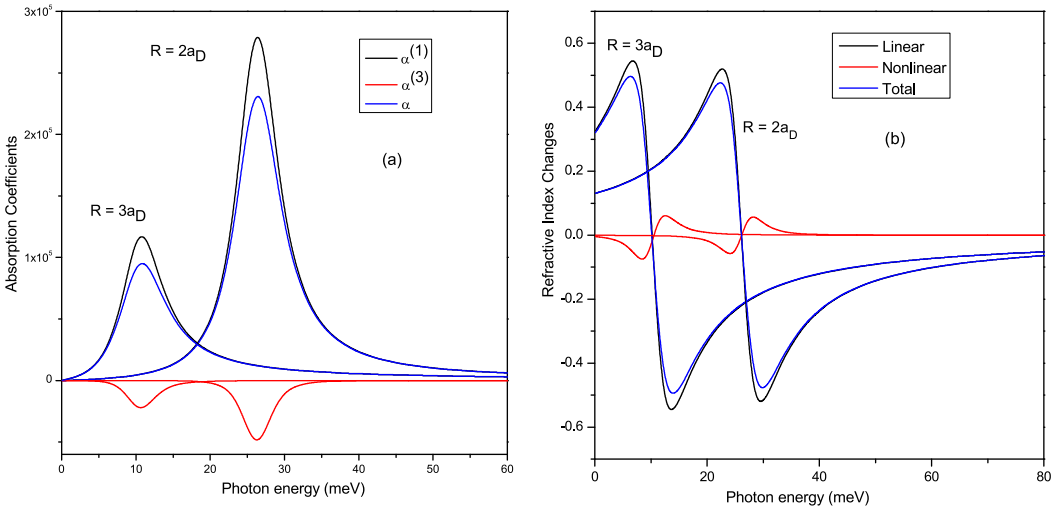

Figure 2. The absorption coefficients (**a**) and the refractive index changes (**b**) as function of incident photon energy $\hbar\omega$ for $R = 2$ and $3\ a_D$.

Now let us turn to the optical responses including the linear, non-linear and total AC and RI related to the $1s - 1p$ transition of (D^+, X) complex. Figure 2a shows the behaviours of the three components of AC versus the incident photon energy $\hbar\omega$ taking into account just the confinement effect. In order to analyse the effect of the confinement on these properties, our calculations are developed for two dot sizes $R = 2\ a_D$ and $3\ a_D$. We see clearly that these components of AC are strongly dependent on the dot size. As it is well known, the (D^+, X) complex energy decreases when the dot size increases, due to the decrease of the Coulomb interactions which leads to a diminishing of the transition energy $E_{fi} = E_{1p} - E_{1s}$. For this reason the curves of the AC show a shift to higher (lower) therahertz frequencies region when the dot size decreases (increases). We remark also that the peaks amplitude increases for strong confinement because the energy difference E_{fi} dominates the tendency of strength of AC. In Figure 2b, the three parts of RI are drawn against the incident photon energy, as in the case of the AC, all components of RI exhibit the same behaviour, they shift to the higher (lower) energies, for large (small) QD sizes. Finally, we should notice that the peaks resonance position are about 6.38 THz and 2.6 THz for $R = 2\ a_D$ and $3\ a_D$ respectively, the importance of these results is that the absorption thresholds are located in the range of the low terahertz frequencies. Thus, the control of the frequencies can be realized by tuning the size of the dots. These results can be exploited in the conception of new optoelectronic devices [51–53], where successful deposition of multi AlAs/GaAs/AlAs spherical quantum dots on substrates (and specifically on graphene) is a key milestone toward the goal to use spherical quantum dots and graphene quantum dots for in situ ultrasensitive terahertz spectroscopy [3,54–56].

To give a good picture of the temperature and pressure effects on the (D^+, X) complex optical responses, we draw in Figure 3a,b the linear and third non-linear and total AC and RI, respectively, versus the incident photon energy $\hbar\omega$ for different values of P and T ($P = 0$, $P = 25$ kbar and $T = 10$, $T = 250$ K). In the case of the pressure effect, we remark that the applied pressure causes an AC shift toward the high value of therahrtz frequencies with an intensities enhancement (Figure 3a). This behaviour was expected because the pressure reinforces the confinement by reducing the $GaAs$ lattice parameter a_0. This dependence of the lattice parameter of $GaAs$ can be modeled by the following formula: $da/dP = -2.6694 \times 10^{-4} a_0$ [57]; so when the pressure is applied the dot size decreases, i.e., the pressure strengths the spatial confinement by shrinking the orbital

wave functions of the three particles (hole, electron and ionized donor) and behaves as an additive confinement and therefore the transition energy E_{fi} increases and consequently a shift of the peaks toward the high value of therahrtz frequencies is observed. On the other hand, and by looking the AC and RI expressions, we see that AC depends on the electric dipole matrix element $|M_{fi}|$, the transition energy E_{fi} and the dielectric constant $\varepsilon(P)$, which are related to the pressure in a different way, so a competition between these quantities appears. Our calculations indicate that the pressure application causes a big change in $\varepsilon(P)$ compared to $|M_{fi}|$ and E_{fi} [26], so the intensities of AC are dominated by the dielectric constant dependent of pressure. Concerning the RI variation (Figure 3b), the same behaviour of AC was found for all components of RI. Regarding the RI amplitudes, we have found a "stability" of intensities when pressure is applied, because RI is independent of $\varepsilon(P)$ [28].

In the case of the influence of the temperature on the AC and RI, we remark that, when the temperature decreases, the curves of AC shift to the higher terahertz frequencies and the peak intensities of AC are reduced (Figure 3a). Indeed, our calculations show that the temperature induces a variation of the electron and hole effective masses and of the band gap energy of $GaAs$, leading to a decrease in energies of the uncorrelated electron-hole-ionized donor, and consequently the energy transition (E_{fi}) decreases. Also we remark that, as the AC situation, the RI (Figure 3b) deeply depend on the temperature; the peaks of RI move to the lower energies region when the temperature increases.

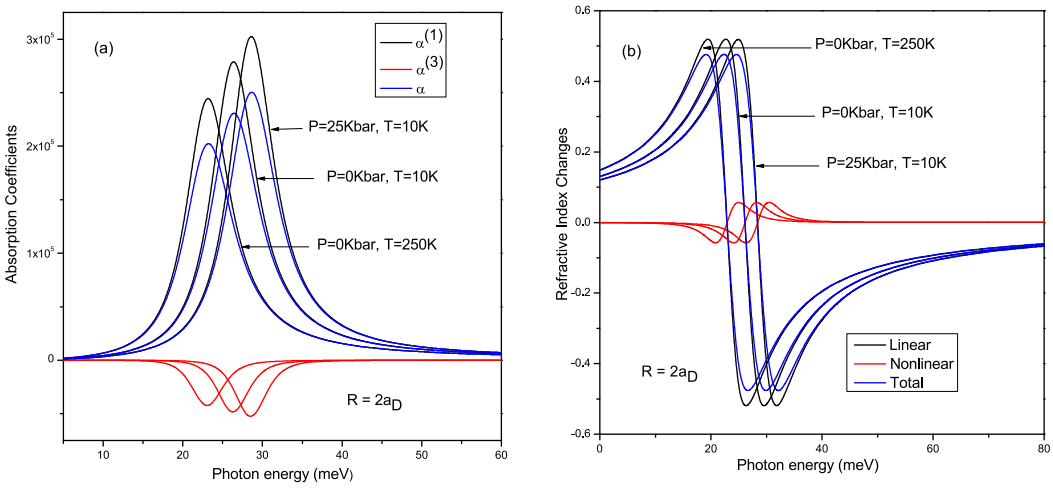

Figure 3. The absorption coefficients (**a**) and the refractive index change (**b**) as function of incident photon energy $\hbar\omega$ for $P = 0, P = 25\ kbar$, $T = 10, T = 250\ K$ and for 2 a_D.

We will finish our investigation with a very important study which is the comparison between the optical responses of the impurity (D^0), the exciton (X) and the (D^+, X) complex. This study is very helpful for the identification of the optical peaks for different materials. To do that, we have followed the same procedures taken to calculate the energies of (D^+, X) complex, by choosing the wave functions given in background theory section (expressions (15)–(18)) corresponding to the exciton and the impurity respectively. In Figure 4a, the absorption coefficients (AC) against the incident photon energy, of the exciton, the impurity and the complex are presented. As we can see, the optical peaks of (D^+, X) complex are located between the exciton peaks (high energy region) and donor impurity (low energy region) i.e the interaction of the donor with the exciton, causes a shift toward THz low frequencies compared to the exciton and a shift to THz higher frequencies compared to the impurity. This behavior is explained by the transition energy difference ($E_{fe} = E_{1p} - E_{1s}$) where: $E_{fe}^{D^0} < E_{fe}^{(D^+,X)} < E_{fe}^{X}$. Figure 4b indicates the variation of the refractive index of X, (D^+, X) and impurity as a function of the energy of incident photon. We notice that the RI behaves in the same way ((D^+, X) complex RI peaks are located between those of exciton and donor impurity) as in the case of AC (Figure 4a).

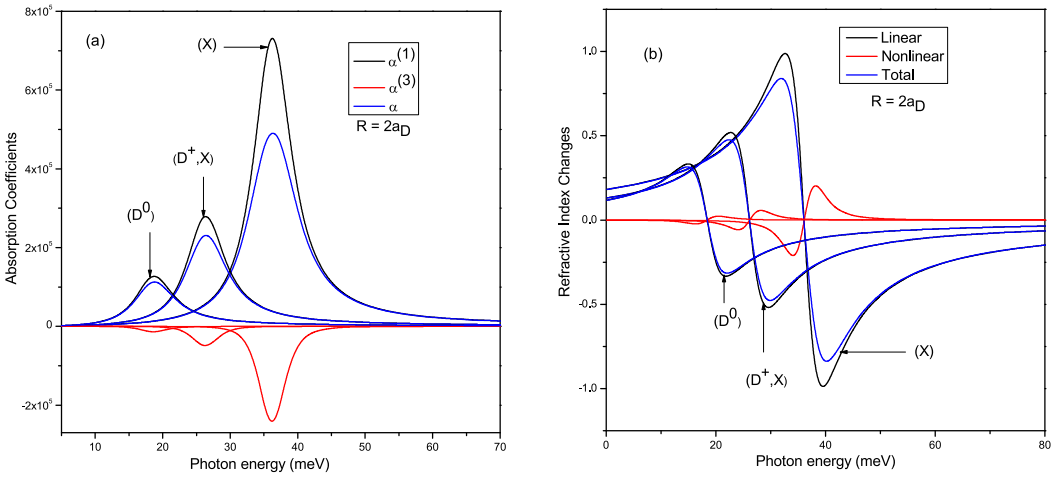

Figure 4. The absorption coefficients (**a**) and The refractive index changes (**b**) against incident photon energy $\hbar\omega$ for exciton, (D^+, X) complex and impurity and for 2 a_D.

4. Conclusions

The binding energy and the optical responses of the (D^+, X) complex depending on the influences of temperature and pressure combined to the size effect, have been investigated. Our results show that the pressure increases the electron-hole and electron-ionized donor attraction, consequently reinforcing the confinement effect. On the other hand, the temperature effect decreases the binding energy due to the electron-hole-ionized donor recombination reinforcing. We also have shown that in the strong confinement regime ($R < 1\ a_D$) the $E^b_{(D^+,X)}$ is less sensitive to both T and P. Also, the optical investigation shows that the AC and the RI depend deeply on the pressure and the temperature as the curves show a shift to higher (lower) therahertz frequencies when the pressure (temperature) increases. These effects can be exploited to change the (D^+, X) optical properties without modifying the radii of QD, but just by controlling the applied pressure and temperature. In a future work it is worthy to investigate the coupling effects between multiple quantum dots and to see how these effects influence the opposite effects caused by temperature and pressure which offer an alternative approach for the adjustment and the control of the optical frequencies. For now, we believe that this study contributes to a better understanding of the (D^+, X) optical properties associated to $1s - 1p$ transitions and to exploit them in different terahertz applications. We have finished our study by a significant comparison between optical properties of (D^+, X) complex, exciton and donor impurity. We have found that the ionized donor's interaction with the exciton causes a shift towards the low energy regions of their optical peaks compared to those of the exciton. These important results can help in the identification of the different optical curves obtained experimentally for different materials and can lead to a novel terahertz detectors concept by controlling size, pressure and temperature.

Author Contributions: Conceptualization,N.A., S.B. and E.M.F.; methodology, N.A.; software, N.A., L.M.P.; formal analysis, N.A. and E.M.F.; resources, L.M.P., D.L.; data curation, N.A.; writing—original draft preparation, N.A., E.M.F.; writing—review and editing, N.A., F.D., E.M.F.; visualization, L.M.P., A.T., D.L., A.E.F., M.E.-Y.; supervision, D.L., S.B., E.M.F.; project administration, E.M.F.; All authors have read and agreed to the published version of the manuscript.

Funding: LMP and DL acknowledge partial financial support from FONDECYT 1180905. AT acknowledges financial support from Postdoctoral Fellowship FONDECYT 3180276. DL acknowledges partial financial support from Centers of excellence with BASAL/ANID financing, AFB180001, CEDENNA.

Data Availability Statement: The data are available from the corresponding author upon reasonable request.

Conflicts of Interest: The authors declare no conflict of interest.

References

1. Bimberg, D.; Grundmann, M.; Ledentsov, N.N. *Quantum Dot Heterostructures*; Wiley: Chichester, UK; New York, NY, USA, 1999.
2. Schmid, G. *Nanoparticles: From Theory to Applications*; Günter Schmid; Wiley VCH Verlag GmbH & Co. KGaA: Weinheim, Germany, 2010.
3. El Fatimy, A.; Myers-Ward, R.L.; Boyd, A.K.; Daniels, K.M.; Gaskill, D.K.; Barbara, P. Epitaxial graphene quantum dots for high-performance terahertz bolometers. *Nat. Nanotech.* **2016**, *11*, 335–338. [CrossRef]
4. Streetman, B.; Banerjee, S. *Solid State Electronic Devices*, 6th ed.; University of Texas: Austin, TX, USA, 2009.
5. Lampert, M.A. Mobile and Immobile Effective-Mass-Particle Complexes in Nonmetallic Solids. *Phys. Rev. Lett.* **1958**, *1*, 450–453. [CrossRef]
6. Skettrup, T.; Suffczynski, M.; Gorzkowski, W. Properties of Excitons Bound to Ionized Donors. *Phys. Rev. B* **1971**, *4*, 512–517. [CrossRef]
7. Stauffer, L.; Stébé, B. Binding energy of ionized-donor-bound excitons in two-dimensional semiconductors. *Phys. Rev. B* **1989**, *39*, 5345–5348. [CrossRef] [PubMed]
8. Stébé, B.; Stauffer, L. Ground state energy of an exciton bound to an ionized donor impurity in two dimensional semiconduc- tors. *Superlattices Microstruct.* **1989**, *5*, 451–453. [CrossRef]
9. Stauffer, L.; and Stébé, B. Ground state energy of an exciton bound to an ionized donor impurity in semiconductor quantum wells. *Solid State Commun.* **1991**, *80*, 983–985. [CrossRef]
10. Dujardin, F.; Feddi, E.; Oukerroum, A.; Bosch Bailach, J.; Martínez-Pastor, J.; Assaid, E. Lateral induced dipole moment and polarizability of excitons in a ZnO single quantum disk. *J. Appl. Phys.* **2013**, *113*, 064314. [CrossRef]
11. Stébé, B.; Assaid, E.; Dujardin, F.; Le Goff, S. Exciton bound to an ionized donor impurity in semiconductor spherical quantum dots. *Phys. Rev. B* **1996**, *54*, 17785–17793. [CrossRef]
12. Feddi, E.; Zouitine, A.; Oukerroum, A.; Dujardin, F.; Assaid, E.; Zazoui, M. Size dependence of the polarizability and Haynes rule for an exciton bound to an ionized donor in a single spherical quantum dot. *J. Appl. Phys.* **2015**, 117, 064309. [CrossRef]
13. Aghoutane, N.; Feddi, E.; El-Yadri, M.; Bosch Bailach, J.; Dujardin, F.; Duque, C.A. Magnetic field and dielectric environment effects on an exciton trapped by an ionized donor in a spherical quantum dot. *Superlattices Microstruct.* **2017**, *111*, 1082–1092. [CrossRef] .
14. Feddi, E.; Aghoutane, N.; El-Yadri, M.; Dujardin, F.; El Aouami, A.; Duque, C.A. Optical and magneto optical responses assigned to probable processes of formation of exciton bound to an ionized donor in quantum dot. *Curr. Appl. Phys.* **2018**, *18*, 452–460. [CrossRef]
15. Karabulut, I.; Baskoutas, S. Linear and nonlinear optical absorption coefficients and refractive index changes in spherical quantum dots: Effects of impurities, electric field, size, and optical intensity. *J. Appl. Phys.* **2008**, *103*, 073512. [CrossRef]
16. Baghramyan, H.M.; Barseghyan, M.G.; Kirakosyan, A.A.; Restrepo, R.L.; Duque, C.A. Linear and nonlinear optical absorption coefficients in $GaAs/Ga_{1-x}Al_xAs$ concentric double quantum rings: Effects of hydrostatic pressureand aluminum concentration. *J. Lumin.* **2013**, *134*, 594–599. [CrossRef]
17. Martinez-Orozco, J.C.; Rodriguez-Magdaleno, K.A.; Suarez, Lopez, J.R.; Duque, C.A.; Restrepo, R.L. Absorption coefficient and relative refractive index change for a double δ-doped GaAs MIGFET-like structure: Electric and magnetic field effects. *Superlattice. Microst.* **2016**, *92*, 166–173. [CrossRef]
18. Karabulut, I.; Mora-Ramos, M.E.; Duque, C.A. Nonlinear optical rectification and optical absorption in $GaAs/Ga_{1-x}Al_xAs$ asymmetric double quantum wells: Combined effects of applied electric and magnetic fields and hydrostatic pressure. *J. Lumin.* **2011**, *131*, 1502–1509. [CrossRef]
19. Yildirim, H.; Tomak, M. Optical absorption of a quantum well with an adjustable asymmetry. *Eur. Phys. J. B* **2006**, *50*, 559–564. [CrossRef]
20. Niculescu, E.C.; Cristea, M. Impurity states and photoionization cross section in CdSe/ZnS core-shell nanodots with dielectric confinement. *J. Lumin.* **2013**, *135*, 120–127. [CrossRef]
21. Owji, E.; Keshavarz, A.; and Mokhtari, H. The effects of temperature, hydrostatic pressure and size on optical gain for GaAs spherical quantum dot laser with hydrogen impurity. *Superlattice. Microst.* **2016**, *98*, 276–282. [CrossRef]
22. Aksahin, E.; Ustoglu Unal, V.; Tomak, M. Exciton related nonlinear optical properties of a spherical quantum dot. *Physica E* **2015**, *74*, 258–263. [CrossRef]
23. Yesilgul, U.; Ungan, F.; Al, E.B.; Kasapoglu, E.; Sari, H; Sökmen, I. Effects of magnetic field, hydrostatic pressure and temperature on the nonlinear optical properties in symmetric double semi-V-shaped quantum well. *Opt. Quantum Electron.* **2016**, *48*, 560. [CrossRef]
24. Kasapoglu, E.; Ungan, F.; Sari, H.; Sökmen, I.; Mora-Ramos, M.E.; Duque, C.A. Donor impurity states and related optical responses in triangular quantum dots under applied electric field. *Superlattice. Microst.* **2014**, *73*, 171–184. [CrossRef]
25. El Haouari, M.; Talbi, A.; Feddi, E.; El Ghazi, H.; Oukerroum, A.; Dujardin, F. Linear and nonlinear optical properties of a single dopant in strained AlAs/GaAs spherical core/shell quantum dots. *Opt. Commun.* **2017**, *383*, 231–237. [CrossRef]
26. Aghoutane, N.; El-Yadri, M.; El Aouami, A.; Feddi, E.; Dujardin, F.; El Haouari, M.; Duque, C.A.; Nguyen, C.V.; Phuc, H.V. Refractive index changes and optical absorption involving 1s-1p excitonic transitions in quantum dot under pressure and temperature effects. *Appl. Phys. A* **2019**, *125*, 17. [CrossRef]

27. Aghoutane, N.; El-Yadri, M.; El Aouami, A.; Feddi, E.; Dujardin, F.; El Haouari, M. Optical Absorption of Excitons in Strained Quasi 2D GaN Quantum Dot. *Phys. Status Solidi* **2019**, *256*, 1800361. [CrossRef]
28. Aghoutane, N.; El-Yadri, M.; El Aouami, A.; Feddi, E.; Long, G.; Sadoqi, M.; Dujardin, F.; Nguyen, C.V.; Nguyen, N.H.; Phuc, H.V. Excitonic nonlinear optical properties in AlN/GaN spherical core/shell quantum dots under pressure. *MRS Commun.* **2019**, *9*, 663–669. [CrossRef]
29. Xie, W. Nonlinear optical properties of an exciton bound to an ionized donor impurity in quantum dots. *Phys. Lett. A* **2011**, *375*, 1213-1217. [CrossRef]
30. Xie, W. Hydrostatic pressure and temperature effects of an exciton-donor complex in quantum dots. *Physica B* **2012**, *407*, 1134–1138. [CrossRef]
31. Dongmei, Z.; Zongchi, W.; Boqi, X. Optical properties of ionized donor-bound excitons confined in strained wurtzite $ZnO/Mg_xZn_{1-x}O$ quantum dots.*J. Semicond.* **2015**, *36*, 033006. [CrossRef]
32. Dallali, L.; Jaziria, S.; and Martínez-Pastor, J. Optical properties of an exciton bound to an ionized impurity in ZnO/SiO_2 quantum dots. *Solid State Commun.* **2015**, *209*, 33–37.
33. Zeng, Z.; Gorgolis, G.; Garoufalis, C.S.; Baskoutas, S. Competition effects of electric and magnetic fields on impurity binding energy in a disc-shaped quantum dot in the presence of pressure and temperature. *Sci. Adv. Mater.* **2014**, *6*, 586–591. [CrossRef]
34. Lopez, S.Y.; Porras-Montenegro, N.; Duque, C.A. Excitons in coupled quantum dots: hydrostatic pressure and electric field effects. *Phys. Status Solidi B* **2009**, *246*, 630. [CrossRef]
35. Duque, C.A.; Lopez, S.Y.; Mora-Ramos, M.E. Hydrostatic pressure effects on the G-X conduction band mixing and the binding energy of a donor impurity in $GaAs/Ga_{1-x}Al_xAs$ quantum wells. *Phys. Status Solidi B* **2007**, *244*, 1964–1970. [CrossRef]
36. Yu, P.Y.; Cordona, M. *Fundamentals of Semiconductors*; Springer: Berlin, Germany, 1998. [CrossRef]
37. Culchac, F.J.; Porras-Montenegro, N.; Latge, A. Hydrostatic pressure effects on electron states in GaAs-(Ga,Al)As double quantum rings. *J. Appl. Phys.* **2009**, *105*, 094324.
38. Barseghyan, M.G.; Mora-Ramos, M.E.; Duque, C.A. Hydrostatic pressure, impurity position and electric and magnetic field effects on the binding energy and photo-ionization cross section of a hydrogenic donor impurity in an InAs Pöschl-Teller quantum ring. *Eur. Phys. J. B* **2011**, *84*, 265–271. [CrossRef]
39. Atanasoff, J.V. The Dielectric Constant of Helium. *Phys. Rev.* **1930**, *36*, 1232–1242. [CrossRef]
40. M'zerd, S.; El Haouari, M.; Talbi, A.; Feddi, E.; Mora-Ramos, M.E. Impact of electron-LO-phonon correction and donor impurity localization on the linear and nonlinear optical properties in spherical core/shell semiconductor quantum dots. *J. Alloys Compound.* **2018**, *753*, 68–78. [CrossRef]
41. Abramowitz, M.; Stegun, I.A. *Handbook of Mathematical Functions: With Formulas, Graphs and Mathematical Tables*; National Bureau of Standards: Washington, DC, USA, 1970. [CrossRef]
42. Harrison, P.; Valavanis, A. *Quantum Wells, Wires and Dots: Theoretical and Computational Physics of Semiconductor Nanostructures*; John Wiley Sons: Hoboken, NJ, USA, 2016.
43. Vahdani, M.R.K.; Rezaei, G. Linear and nonlinear optical properties of a hydrogenic donor in lens-shaped quantum dots. *Phys. Lett. A* **2009**, *373*, 3079–3084.
44. Jafari, A.R. Optical properties of hydrogenic impurity in an inhomogeneous infinite spherical quantum dot. *Physica B***2015**, *456*, 72–77. [CrossRef]
45. Abraham, J.; Hudson, M.; John Peter, A. Dielectric confinement on exciton binding energy and nonlinear optical properties in a strained $Zn_{1-x}Mg_xSe/Zn_{1-x}Mg_xSe$ quantum well. *J. Semicond.* **2012**, *33*, 9. [CrossRef]
46. Baghramyan, H.M.; Barseghyan, M.G.; Laroze, D. Molecular spectrum of laterally coupled quantum rings under intense terahertz radiation. *Sci. Rep.* **2017**, *7*, 10485.
47. Baghramyan, H.M.; Barseghyan, M.G.; Kirakosyan, A.A.; Ojeda, J.H.; Bragard, J.; Laroze, D. Modeling of anisotropic properties of double quantum rings by the terahertz laser field. *Sci. Rep.* **2018**, *8*, 6145. [CrossRef]
48. Barseghyan, M.G.; Mughnetsyan, V.N.; Pérez, L.M.; Kirakosyan, A.A.; Laroze, D. Effect of the impurity on the Aharonov-Bohm oscillations and the intraband absorption in $GaAs/Ga_{1-x}Al_xAs$ quantum ring under intense THz laser field. *Physica E* **2019**, *111*, 91-97. [CrossRef]
49. Barseghyan, M.G.; Mughnetsyan, V.N.; Baghramyan, H.M.; Ungan, F.; Pérez, L.M.; Laroze, D. Control of electronic and optical properties of a laser dressed double quantum dot molecule by lateral electric field. *Physica E* **2021**, *126*, 114362. [CrossRef]
50. John Peter, A. The effect of hydrostatic pressure on binding energy of impurity states in spherical quantum dots. *Physica E* **2005**, *28*, 225–229. [CrossRef]
51. Cheon, H.; Yang, H.; Lee, S.; Kim, Y.; Son, J. Terahertz molecular resonance of cancer DNA. *Sci. Rep.* **2016**, *6*, 37103. [CrossRef]
52. Kampfrath, T.; Tanaka, K.; Nelson, K. Resonant and nonresonant control over matter and light by intense terahertz transients. *Nat. Photon* **2013**, *7*, 680–690. [CrossRef]
53. Sengupta, K.; Nagatsuma, T.; Mittleman, D.M. Terahertz integrated electronic and hybrid electronic-photonic systems. *Nat. Electron.* **2018**, *1*, 622–635. [CrossRef]
54. St Marie, L.; El Fatimy, A.; Hrubý, J.; Nemec, I.; Hunt, J.; Myers-Ward, R.; Gaskill, D.K.; Kruskopf, M.; Yang, Y.; Elmquist, R. Nanostructured graphene for nanoscale electron paramagnetic resonance spectroscopy. *J. Phys. Mater.* **2020**, *3*, 14013. [CrossRef]
55. El Fatimy, A.; Nath, A.; Kong, B.D.; Boyd, A.K.; Myers-Ward, R.L.; Daniels, K.M.; Jadidi, J.; Murphy, T.E.; Gaskill, D.K.; Barbara, P. Ultra-broadband photodetectors based on epitaxial graphene quantum dots. *Nanophotonics* **2017**, *7*, 735–740.

56. El Fatimy, A.; Han, P.; Quirk, N.; Marie, S.; Dejarld, M.T.; Myers-Ward, R.; Daniels, K.; Pavunny, S.; Gaskill, D.K.; Aytac, Y.; et al. Effect of defect-induced cooling on graphene hot-electron bolometers. *Carbon* **2019**, *154*, 497–502. [CrossRef]
57. Benedictal, A.; Sukumar, B.; Navaneethakrishnan, K. Pressure dependent donor ionization energies in quantum-well. *Phys. Status Solidi* **1993**, *178*, 167–172. [CrossRef]